DETERMINATION OF SUPERCAVITY SHAPE FOR AXISYMMETRIC CAVITATORS AT DIFFERENT NON-ZERO ATTACK ANGLES, USING BOUNDARY ELEMENT METHOD

R. Shafaghat *

Department of Mechanical Engineering
NIT, Iran

S. M. Hosseinalipour

Department of Mechanical Engineering
IUST, Iran

A. Vahedgermi

Department of Mechanical Engineering
IUST, Iran

ABSTRACT

When fluid passes a cavitator in the supercavitating flow, a supercavity forms behind the cavitator. Variation of the cavitator attack angle can influence theshape of the formed supercavity behind the cavitator. Consequently, it will affect the stability of supercavity behind the supercavitating cavitator with after body. In this study, a direct boundary element method (DBEM) is being formulated and numerically solved for3D unbounded potential flowspassing supercavitating bodies of revolution at different attack angles. In the analysis of potential flows passing supercavitating bodies at non-zero attack angles, a cavity closure model must be employed in order to close the mathematical formulationand guarantee the solution uniqueness. In the present study, we employ modified Riabouchinsky closure model. Since the location of the cavity surface is unknown at prior, an iterative scheme is used and for the first stage, an arbitrary cavity surface is assumed. The flow field is then solved and by an iterative process, the location of the cavity surface is corrected. Upon convergence, the exact boundary conditions are satisfied on the body-cavity boundary. A powerful CFD codeis developed to solve the 3D supercavitating flows behind all types of axisymmetric cavitators (such as disk, cone, *etc*) at zero and non-zero attack angles. The predictions of the CFD code are compared with those generated by verified existing data. The predictions of the code for supercavitating cones and disks seem to be excellent. Using the obtained data from CFD code, we investigate the supercavity shapesand corresponding stability at different attack angles with a fixed cavitation number.

Keywords: Boundary element method, Supercavitating flows, Cavitator, Cavity closure, Cavitation number, 3D, Attack angle.

1. INTRODUCTION

Supercavitation is a revolutionary means to achieve drag reduction up to 90% on an underwater body [1]. This level of drag reduction will have dramatic effects on the operation of naval forces. The high level of drag reduction is achieved by enveloping the body within a gaseous cavity. Only small area at the nose (cavitator) remains in contact with the liquid.

The study of axisymmetric and three-dimensional supercavitating flow problems has always been of great interest, since they are in general more applicable to reality than two dimensional models. Of the early work on infinite-length axisymmetric supercavitating flow, we note Reichardt [2], who experimentally studied the axisymmetric supercavitating flows, and Garabedian [3], who developed an analytical method for calculating cavity shapes, though the accuracy of the method he presented is limited. Following the work on axisymmetric flow by Reichardt [2] and Garabedian [3], attention was paid to finite-length cavities springing from bodies of revolution by a number of authors, such as Cuthbert and Street [4], Brennen [5], Chou [6], Aitchison [7], Hase [8] and Varghese, Uhlman and Kirschner [9]. These authors used a variety of techniques for modeling the supercavitating flows including finite difference, finite element, boundary integral and interior source methods. Ingber presented a numerical modelling (BEM) in order to calculate a partially cavitation behind a body of revolution with after body and at zero and non-zero angle of attack [10].

The most useful information from a solution of a

* Corresponding author (rshafaghat@nit.ac.ir)

DOI : 10.1017/jmech.2012.44
Copyright © 2012 The Society of Theoretical and Applied Mechanics, R.O.C.
https://doi.org/10.1017/jmech.2012.43 Published online by Cambridge University Press

supercavitating flow problem is the spatial location of the free surface (cavity surface) and knowledge of velocities and/or pressures along the boundaries. This realization leads one to feel that domain-type techniques (such as FDM and FEM) are computationally inefficient and that the problem is ideally suited to a boundary element method (BEM) solution [11].

The boundary element method is based on the descritization of an integral equation that, mathematically, is equal to the governing partial differential equation of the problem. The one of the main advantages of the boundary element method is that in which, instead of the whole domain, we generate the mesh only on the boundaries of the domain and so, the number of the generated meshes reduces considerably. This advantage decreases the numerical solution run-time and solution costs [12].

At literatures such as [11], [13] and [14] the authors deducedthat for supercavitating flows, the BEM gives more accurate solutions than finite difference or finite element methods. Moreover, the method can, in most cases, provide an order of magnitude increase in efficiency over finite difference or finite element methods. As mentioned before, the gain in efficiency and ease of use is due to the fact that solution of thepartial differentialequation in the entire domain is reduced to the solution of an integral equation on the boundary of the domain.

In this study, we present a formulation of direct boundary element method for finding numerical solutions to 3D supercavitating flows involving finite-lengthsupercavities. An example of such supercavity is shown in Figs. 1 and 2, where we illustrate finite-length cavities with modified Riabouchinsky closure models behind a cone. It should be noted that this closure model has been chosen as a compromise between simplicity and physically validity [15]. According to the modified Riabouchinsky closure model, an image disk is introduced at a certain distance downstream of the real body (cavitator) to make the cavity closed. Application of this closure model for the axisymmetric boundary-element method is discussed in detail in Kirschner *et al*. [16]. Since the location of the cavity surface is unknown at prior, an iterative scheme is used. Where, for the first stage, an arbitrary cavity surface is assumed. The flow field is then solved and by an iterative process, the location of the cavity surface is corrected. Upon convergence, the exact boundary conditions are satisfied on the body-cavity boundary. The iterative scheme for determining the cavity surface position is similar to that of references [17-19].

A powerful CFD code is developed to solve the 3D supercavitating flows behind all types of axisymmetric cavitators (such as disk, cone, *etc*) at zero and non-zero attack angle. The predictions of the CFD code are compared with those generated by existing supercavitation software data. The predictions of code for supercavitating cones and disks are seen to be excellent. The main goal of this study is to investigate the influence of the attack angle variation in the cavity shape and supercavity stability with a fixed cavitation number.

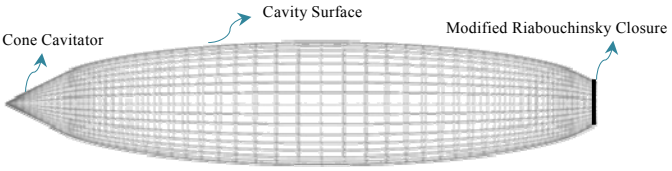


Fig. 1 Side view of finite-length supercavity with modified Riabouchinsky closure model

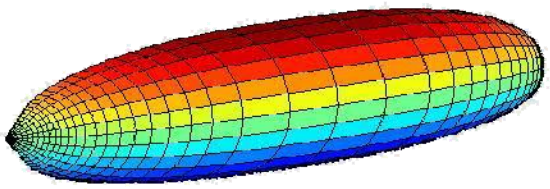


Fig. 2 Isometric view of finite-length supercavity with modified Riabouchinsky closure model

2. POTENTIAL FLOW FORMULATION

Consider the unbounded, steady and irrotational flow of an inviscid and incompressible liquid past a supercavitating cone placed at non-zero attack angle in the flow direction (Fig. 3). The flow is then a potential flow and hence possesses a potential function, Φ, which in the fluid satisfies Laplace's equation:

$$\nabla^2\Phi = \frac{\partial^2\Phi}{\partial x^2} + \frac{\partial^2\Phi}{\partial y^2} + \frac{\partial^2\Phi}{\partial z^2} = 0 \tag{1}$$

The potential function can be subdivided into two parts: One part due to the free stream, φ_{fs}, and the other part due to the perturbation caused by the body and cavity, φ_p. The potential function due to the free stream, φ_{fs}, can be calculated as follow:

$$\varphi_{fs} = \vec{U}_\infty \cdot \vec{R}$$

where, $\vec{U}_\infty$ is the freestream velocity vector and $\vec{R}$ is the position vector.

So, the potential function due to the perturbation caused by the body and cavity, φ_p, can be defined from the total potential by:

$$\Phi = \vec{U}_\infty \cdot \vec{R} + \varphi_p \tag{2}$$

So that the disturbance velocity is given by the gradient of the disturbance potential, the disturbance potential also obeys the Laplace's equation:

$$\nabla^2\varphi_p = \frac{\partial^2\varphi_p}{\partial x^2} + \frac{\partial^2\varphi_p}{\partial y^2} + \frac{\partial^2\varphi_p}{\partial z^2} = 0 \tag{3}$$

3. BOUNDARY CONDITIONS

The requirement that the flow be tangential to the cavity and body surface (S_c and S_b) gives the following kinematic condition on the body-cavity surface, $S = S_c + S_b$:

https://doi.org/10.1017/jmech.2012.43 Published online by Cambridge University Press

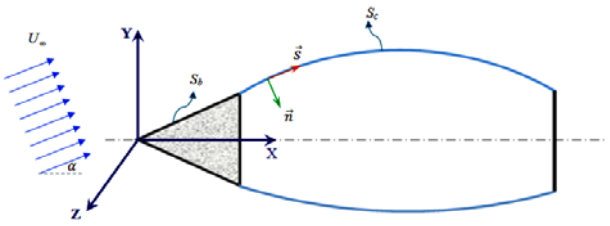


Fig. 3 Typical problem geometry

$$\frac{\partial \Phi}{\partial \vec{n}} = 0 \quad \text{on } S. \tag{4}$$

where, $\vec{n}$ is the unit vector normal to the body-cavity surface (see Fig. 3). Combining Eq. (2) with (4) gives:

$$\frac{\partial \varphi_p}{\partial \vec{n}} = -\frac{\partial (\vec{U}_\infty \cdot \vec{R})}{\partial \vec{n}} \quad \text{on } S. \tag{5}$$

Similarly, a dynamic boundary condition (constant pressure or constant velocity) must be applied on the cavity surface, S_c. Using Bernoulli's equation, it may be shown that this condition becomes:

$$U_c = U_\infty \sqrt{1+\sigma} \quad \text{on} \quad S_c \tag{6}$$

where, σ is the cavitation number and U_c is the constant representing the liquid velocity along the cavity surfacethatcan be calculated as follow:

$$U_c = \sqrt{\left(\frac{\partial(\varphi_p + \vec{U}_\infty \cdot \vec{R})}{\partial x}\right)^2 + \left(\frac{\partial(\varphi_p + \vec{U}_\infty \cdot \vec{R})}{\partial y}\right)^2 + \left(\frac{\partial(\varphi_p + \vec{U}_\infty \cdot \vec{R})}{\partial z}\right)^2} \tag{7}$$

Combining Eq (7) with (6) gives:

$$\sqrt{\left(\frac{\partial(\varphi_p + \vec{U}_\infty \cdot \vec{R})}{\partial x}\right)^2 + \left(\frac{\partial(\varphi_p + \vec{U}_\infty \cdot \vec{R})}{\partial y}\right)^2 + \frac{\partial(\varphi_p + \vec{U}_\infty \cdot \vec{R})}{\partial z}} = U_\infty \sqrt{1+\sigma} \quad \text{on} \quad S_c \tag{8}$$

4. DIRECT BOUNDARY ELEMENT METHOD FORMULATION

The problem governed by Eqs. (3), (5) and (8) is highly nonlinear not only because the dynamics boundary condition represents a nonlinear boundary condition but also because the position of the cavity surface is unknown at prior. Since this position is of primary concern, the DBEM is well suited for this problem.In the DBEM formulation, a boundary integral equation (BIE) is derived from Laplace's equation (Eq. 3) through application of Green's second theorem. In 3D flow, it has the following form:

$$\iint_S \left[\varphi_p(\vec{R}) \frac{\partial G(\vec{R}, \vec{R}_0)}{\partial \vec{n}} - G(\vec{R}, \vec{R}_0) \frac{\partial \varphi_p(\vec{R})}{\partial \vec{n}} \right] dS(\vec{R}) = -\frac{1}{2} \varphi_p(\vec{R}_0) \tag{9}$$

where, $\vec{n}$ is the unit vector normal to the body-cavity surface, $\vec{R}_0$ is the position vector of an interior 'load' point or 'source' point with coordinates (x_p, y_p, z_p), $\vec{R}$ is the position vector of a 'field' point with coordinates (x_o, y_o, z_o) and $\partial G(\vec{R}, \vec{R}_0)/\partial \vec{n}$ and $G(\vec{R}, \vec{R}_0)$ are the first and second kernels respectively and defined as follows:

$$\frac{\partial G(\vec{R}, \vec{R}_0)}{\partial \vec{n}} = -\frac{1}{4\pi r^2} \frac{\partial r}{\partial \vec{n}} = \frac{-1}{4\pi |\vec{R} - \vec{R}_0|^3} (\vec{R}, \vec{R}_0) \cdot \vec{n} \tag{10}$$

$$G(\vec{R}, \vec{R}_0) = -\frac{1}{4\pi r} = \frac{1}{4\pi |\vec{R} - \vec{R}_0|} \tag{11}$$

5. NUMERICAL SOLUTION

To solve the three-dimensional potential BIE numerically, the body-cavity surface is discretized intoa number of connected elements. The discretization of the body-cavity surface is accomplished with rays in the direction of the axis of the body and transverse rings (Fig. 2). Previous experiences of BEM users have established that in most three-dimensional problem analysisapplications, isoparametricquadratic elements provide the best compromise between accuracy andefficiency [12]. In three-dimensional problems, it is convenient to divide the surface into quadrilateral elements with a quadratic curve on each side. Since three nodes are needed for a quadratic curve, the total number of nodes in each element is eight. We can introduce two local (intrinsic) variables ξ_1 and ξ_2 with their origins at the center of the element and limiting values of −1 and +1 at the outer edges (see Fig. 4).

Therefore, the geometry of an element can be described by the coordinates of its eight nodes and shape function as follows:

$$\begin{aligned} X^j(\xi_1, \xi_2) &= \sum_{c=1}^{8} N_c(\xi_1, \xi_2)\, x_c^j \\ Y^j(\xi_1, \xi_2) &= \sum_{c=1}^{8} N_c(\xi_1, \xi_2)\, y_c^j \\ Z^j(\xi_1, \xi_2) &= \sum_{c=1}^{8} N_c(\xi_1, \xi_2)\, z_c^j \end{aligned} \tag{12}$$

Note that, in the above equations, x_c^j, y_c^j, z_c^j is the coordinates of the c^{th} node of the j^{th} element and (X^j, Y^j, Z^j) is the coordinates of the any point on the j^{th} element. The shape functions $N_c(\xi_1, \xi_2)$ must satisfy two conditions:

1. $N_c(\xi_1, \xi_2) = 1$ at node c
2. $N_c(\xi_1, \xi_2) = 0$ at all other nodes

https://doi.org/10.1017/jmech.2012.43 Published online by Cambridge University Press

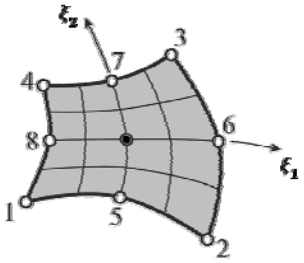


Fig. 4 Three-dimensional isoparametric quadrilateral quadratic element

Using above conditions, the shape functions can be explicitly written in terms of intrinsic coordinates ξ_1 and ξ_2.

The BIE of Eq. (9) cannow be written in terms of the local coordinates ξ_1 and ξ_2 as follows:

$$\sum_{j=1}^{N}\left[\frac{(\varphi_p)_j\,\delta_{ij}}{2}+\sum_{c=1}^{8}(\varphi_p)_j\int_{-1}^{1}\int_{-1}^{1}\frac{\partial G_{ij}(P_i,\xi_1,\xi_2)}{\partial\vec{n}_j}N_c(\xi_1,\xi_2)\,J(\xi_1,\xi_2)d\xi_1\,d\xi_2\right]$$
$$=\sum_{j=1}^{N}\sum_{c=1}^{8}\int_{-1}^{1}\int_{-1}^{1}\left(\frac{\partial\varphi}{\partial\vec{n}}\right)_j G_{ij}(P_i,\xi_1,\xi_2)\,N_c(\xi_1,\xi_2)J(\xi_1,\xi_2)\,d\xi_1\,d\xi_2 \tag{13}$$

$$\delta_{ij}=\begin{cases}1 & \text{if} \quad i=j\\ 0 & \text{if} \quad i\neq j\end{cases} \tag{14}$$

The symbol G_{ij} means the Green's function with the source point at the centroid of the i^{th} element and with the field point varying over all locations in the j^{th} element as the integration is carried out. The symbol $J(\xi_1, \xi_2)$ is the Jacobian of the transformation due to transformation of the variable from the surface to the intrinsic coordinates ξ_1 and ξ_2. In the above discretized equation, the only unknowns are the values of φ_p on the N element centroids. So, there will be N equations.

Define:

$$A_{ij}=\frac{\delta_{ij}}{2}+\sum_{c=1}^{8}\int_{-1}^{1}\int_{-1}^{1}\frac{\partial G_{ij}(P_i,\xi_1,\xi_2)}{\partial\vec{n}_j}N_c(\xi_1,\xi_2)\,J(\xi_1,\xi_2)\,d\xi_1\,d\xi_2 \tag{15}$$

and

$$B_i=\sum_{j=1}^{N}\sum_{c=1}^{8}\int_{-1}^{1}\int_{-1}^{1}\left(\frac{\partial\varphi_p}{\partial\vec{n}}\right)_j G_{ij}(P_i,\xi_1,\xi_2)N_c(\xi_1,\xi_2)\,J(\xi_1,\xi_2)\,d\xi_1\,d\xi_2 \tag{16}$$

Then, the final set of equations for the N values of φ_p is:

$$\sum_{j=1}^{N}A_{ij}(\varphi_p)_j=B_i\Rightarrow A\varphi_p=B \tag{17}$$

For the numerical solution of the problem, we guess an initial cavity surface location (see Fig. 5). Then the body-cavity surface, S, is subdivided into a number of elements (see Fig. 6). The mesh concentration is higher near the cavity surface detachment and reattachment zones because of singularity in these zones.

The DBEM solution then produces the values of disturbance potential, φ_p, at thecentroid nodes of the boundary elements. The central problem is calculation of the velocity at the body-cavity surface. At each element, the total flow is tangent to the body-cavity surface so we need only find tangential velocity. The tangential velocity is the tangential derivative of the total potential, Φ (perturbation potential plus any exterior potential for the steady flow problems we have been considering). We know how to determine the tangential derivative at a point using a modified central difference procedure for smooth objects. Even when the object has a sharp edge (detachment and reattachment zones) or tip, this procedure can be used for all central nodes of elements except for those adjacent to a sharp edge and tip. In addition, the numerical derivative can be determined at a point that is midway between the first and second central nodes from the sharp edge (and tip). Then the tangential derivative can be approximated at a central node nearest the sharp edge (and tip) by numerical extrapolation. The obtained values for velocity at central nodes of elements on the cavity surface are all equal for the correct cavity surface position shown in Fig. 5 (but, of course, not for the assumed one), and it is essential that a procedure be devised to properly move the cavity surface in the steps of the iteration scheme so that the constant-velocity or constant pressure condition bemore closely satisfied on the moved surface. The iterative scheme here is the one employed by Shafaghat *et al*. [17-19]. It should be noted thatthe convergence of the iteration is dependent on the initial guessedsurfacefor the location of the cavity boundary surface. In fact, if the initial guessis poor, the iteration may not converge at all. Therefore, it is beneficial to have a method for generating the initial guess for the cavity surface, capable of reducing the computational costs. In this work, the initial guess for the cavity surface is generated by considering the points of cavity surface detachment and cavity surface reattachment and then fitting an arc of a circle through these points, which is tangent to the body at detachment point (each ray is an arc of a circle).

6. ITERATION PROCEDURE

According to the previous subsection, the iteration procedure will be as follows:

(i) Assume an initial cavity surface location.

(ii) DBEM solution provides value of velocity at central node of each cavity surfaceelement (q_{c_i}).

(iii) Calculate the displacement of each element (in direction of unit normal vector of each element), using the following empirical relation:

https://doi.org/10.1017/jmech.2012.43 Published online by Cambridge University Press

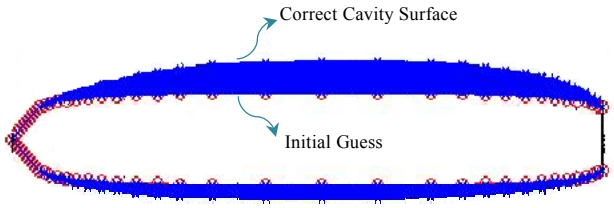


Fig. 5 Side cross section of discretized body-cavity surface

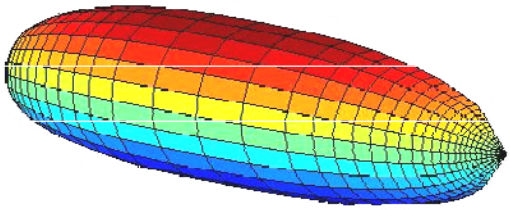


Fig. 6 Discretized body-cavity surface

$$\Delta r_i = \omega \frac{|500q_S^2 - 500q_{C_i}^2|}{1000} r_i^3 \tag{18}$$

where ω is a relaxation parameter, q_{c_i} is the value of velocity at central node of i^{th} elementof the cavity surfaceand q_s is the value of velocity at separation point.

(iv) Compute the relative norm of increments

$$Norm = \sum_{i=1}^{N} \frac{1}{N} \left| \frac{r_i^{k+1} - r_i^k}{r_i^k} \right| \tag{19}$$

where N is the number of cavity surfaceelements. If the norm is smaller than a specified tolerance ε, the process has converged and is terminated; otherwise, the cavity surface is moved to a new location given by $r_i^{k+1} = r_i^k + \omega \Delta r_i^{k+1}$ and the process returns to step (ii).

7. RESULTS DISCUSSION

In order to obtain the final results, the cavitator and cavity dimensions, closure model properties and different attack angles are presented in Table 1.

Since there isno qualified experimentaldatato verify the obtained results, the 3D coderesults are verified bythe results of the other similar solutions at zero attack angles. We compared the results with the results of the existing verified axisymmetric supercavitation software [19,20]. As you see in Figs. 7 and 8, the accuracy of the 3D code results is acceptable.

After verifying the results, we solved the 3D supercavitation problem at non-zero attack angles. In order to investigate the results of 3D supercavitating flows, it should be noted that in a fixed infinity conditions (P_∞ & U_∞), cavitation number doesn't change with different attack angles. With respect to iterative procedure,

Table 1 Final solution conditions

Main properties	Description
Cavitator type	Cone
Cone head angle (degree)	90
Cavitator diameter	1
Cavity dimensionless lengths	5, 10, 15 and 20
Cavity closure model	Modified Riabouchinsky
Disc diameter (in closure region)	1
Attack angles (degree)	0, 1, 3, 5 and 10

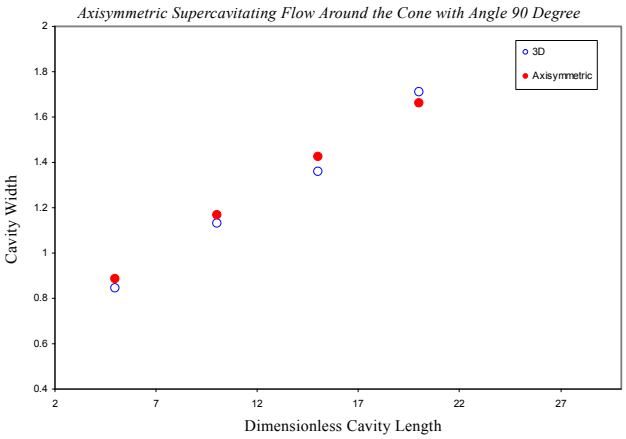


Fig. 7 Cavity widths for cavities of various lengths

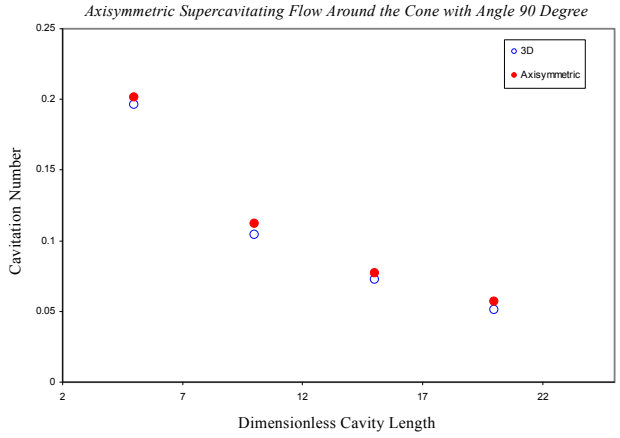


Fig. 8 Cavitation numbers for cavities of various lengths

supercavity shapes are obtained at a known cavity length. So, at a fixed cavitation number and cavity length, the supercavity geometric characteristics are obtained for different attack angles. Figure 9 shows the sample results for $1/d = 10$.

As you see in Fig. 9, by increasing the attack angle, the cavity shape deviates toward flow direction. In order to describe thesupercavity behavior at different attack angles, the cavity width characteristic, (t_u / t_d), is introduced (see Fig. 10).

https://doi.org/10.1017/jmech.2012.43 Published online by Cambridge University Press

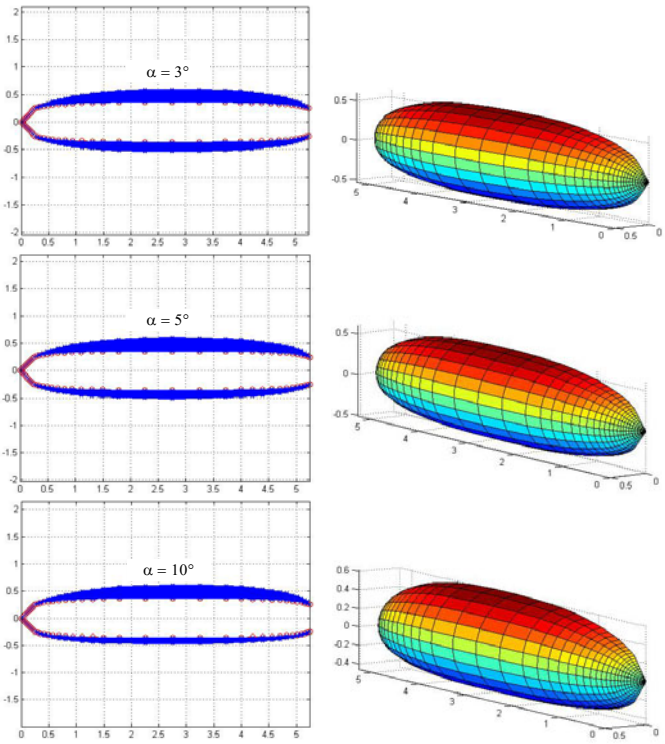


Fig. 9 Sample results for $l/d = 10$

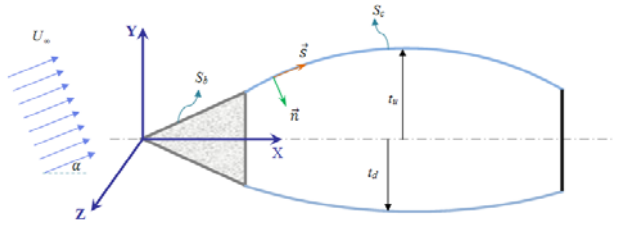


Fig. 10 Cavity width characteristics definition

Variation of the cavity width characteristicsby changing the attack angle at different dimensionless cavity lengths arepresented in Table 2 and Fig. 11.

Any disturbances destroying the supercavity shape may cause the motion path deviation. An important question in supercavitating body motion is that do these bodies can keep their way toward the target after imposing a non-zero attack angle?So, an important problem is the control strategy in supercavitating bodies. By increasing the attack angle, the cavity shape deviates toward the flow direction. When dimensionless cavity length is large (in supercavitation state), changing of the cavity width characteristics is notable. In this condition cavity surface cuts the after body surface and then pressure distribution on the after body surface will change. So, supercavity in a supercavitating case with after body will be unstable by changing the attack angle (Fig. 12).

8. CONCLUSIONS

In this study, the supercaviy shapes at zero and non-zero attack angles of axisymmetric cavitators are investigated. We can present the final conclusion as follows:

Table 2 Cavity width characteristics for various attack angles and various dimensionless cavity lengths

Attack Angle (Degree)	(t_u/t_d)			
	$l/d = 5$	$l/d = 10$	$l/d = 15$	$l/d = 20$
0	1	1	1	1
1	1.016551	1.039178	1.047005	1.078987
3	1.047842	1.111049	1.135733	1.208316
5	1.076845	1.175322	1.204178	1.316214
10	1.143427	1.315936	1.348859	1.515203

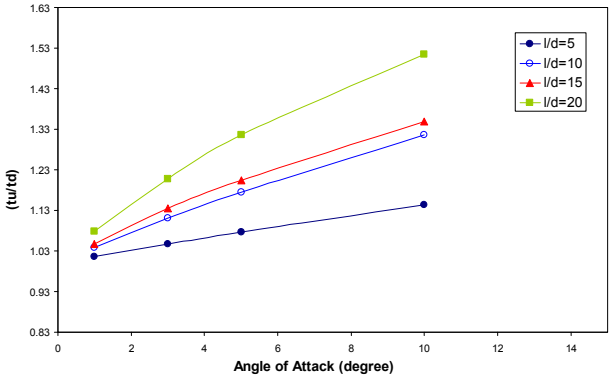


Fig. 11 Cavity width characteristics for various attack angles and various dimensionless cavity lengths

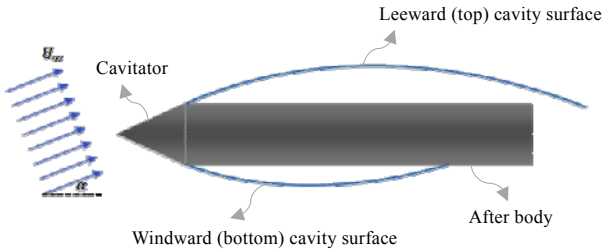


Fig. 12 Schematic of supercavity formed behind a supercavitating case with after body

1. Direct BoundaryElement Method (DBEM) can be a suitable method in order to investigation the 3D supercavitating flows.
2. It should be noted that the convergence of the iteration is dependent on the initial guessed surface for the location of the supercavity boundary surface.
3. In 3D supercavitation problems, isoparametric quadratic elements provide the best compromise between accuracy and efficiency.
4. By increasing the attack angle, the supercavity shape deviates toward the flow direction. When dimensionless cavity length is large (in supercavitation state), changing of the cavity width characteristics is notable. In this condition, supercavity surface cuts the after body surface and then pressure distribution on the after body surface will change. So, supercavity in a supercavitating case with after body will be unstable by changing the attack angle.

https://doi.org/10.1017/jmech.2012.43 Published online by Cambridge University Press

REFERENCES

1. Kuklinski, R., Henoch, C. and Castano, J., "Experimental Study of Ventilated Cavities on Dynamic Test Model," *Naval Undersea Warfare Center.*, Cav2001: Session B3.004 (2001).
2. Reichardt, H., "The Physical Laws Governing the Cavitation Bubbles Produced Behind Solids of Revolution in a Fluid Flow," *The Kaiser Wilhelm Institute for Hydrodynamic Research.*, Gottingen, Rep. UM 6628, (1945).
3. Garabedian, P. R., "The Calculation of Axially Symmetric Cavities and Jets," *Pacific Journal of Mathematics*, **6**, pp. 611–689 (1956).
4. Cuthbert, J. and Street, R., "An Approximate Theory for Supercavitating Flow About Slender Bodies of Revolution," *LMSC Report TM81-73/39*, Lockheed Missiles and Space Co., Sunnyvale,California, (1964).
5. Brennen, C. A., "Numerical Solution of Axisymmetric Cavity Flows," *Journal of Fluid Mechanics*, **37**, p. 4, 671–688 (1969).
6. Chou, Y. S., "Axisymmetric Cavity Flows Past Slender Bodies of Revolution," *Journal of Hydronautics*, **8**, pp. 13–18 (1974).
7. Aitchison, J. M., "The Numerical Solution of Planar and Axisymmetric Cavitational Flow Problems," *Computers and Fluids*, **12**, pp. 55–65 (1984).
8. Hase, P. M., "InteriorSource Methods for Planar and Axisymmetric Supercavitating Flows," *Thesis Submitted for the Degree of Doctor of Philosophy*, (2003).
9. Verghese, A. N., Uhlman, J. S. and Kirschner, I. N., "Numerical Analysis of High – Speed Bodies in Partially Cavitation Axisymmetric Flow, Transactions of ASME," *Journal of Engineering*, **127**, pp. 41–54 (2005).
10. Ingber, M. S. and Halley, C. E., "Numerical Modelling of Cavities on Axisymmetric Bodies at Zero and Non-Zero Angle of Attack'," *International Journal of Numerical Method in Fluid*, **15**, pp. 251–271 (1992).
11. Wrobel, L. C., "A Simple and Efficient BEM Algorithm for Planar Cavity Flows," *International Journal for Numerical Methods in Fluids*, **14**, pp. 524–537 (1992).
12. Becker, A. A., *The Boundary Element Method in Engineering*, McGraw-Hill Book Company (1992).
13. Kennon, S. R., "Boundary Element Method," *Graduate Research Assistant, Department of Aerospace Engineering and Engineering Mechanics*, University of Texas at Austin, Austin, TX. (1986).
14. Mukherjee, S. and Morjaria, M., "On the Efficiency and Accuracy of the Boundary Element Method," *International Journal for Numerical Methods in Engineering*, **20**, pp. 515–522 (1984).
15. Kirschner, I. N., Fine, N. E., Uhlman, J. S. and Kring, D. C., "Numerical Modeling of Supercavitating Flows," Paper presented at the RTO AVT lecture series on "Supercavitating Flows", held on the Von Karman Institute (VKI) in Belgium, and published in RTO EN-010, 12–16 (2001).
16. Kirschner, I. N., Uhlman, J. S., Varghese, A. N. and Kuria, I. M., "Supercavitating Projectiles in Axisymmetric Subsonic Liquid Flows," *Proceedings of the ASME & JSME Fluids Engineering Annual Conference & Exhibition, Cavitation and Multiphase Flow Forum*, FED 210, J. Katz and Y. Matsumoto, editors, Hilton Head Island, SC (1995).
17. Shafaghat, R., Hosseinalipour, S. M. and Shariatifard, A., "Numerical Analysis of a Two Dimensional Bounded Supercavitation Flow, 15th Annual Conferences of the CFD Society of Canada," *Toronto*, Canada, May 27-31 (2007).
18. Shafaghat, R., Hosseinalipour, S. M. and Shariatifard, A., "Numerical Analysis of Two-Dimensional Supercavitation Flow Using a Boundary Element Method," *Journal of Numerical Simulations in Engineering*, University of Mazandaran. **3**, pp. 216–223 (2008).
19. Shafaghat, R., Hosseinalipour, S. M., Nouri, N. M. and Vahedgermi, A., "Mathematical Approach to Investigate the Behavior of the Principal Parameters in Axisymmetric Supercavitating Flows, Using Boundary Element Method," *Journal of Mechanics*, **25**, pp. 465–473 (2009).
20. Shafaghat, R., Hosseinalipour, S. M. and Vahedgermi, A., "Numerical Analysis of Axisymmetric Supercavitating Flows," Using Boundary Element Method, 11th Fluid Dynamics Conference, K. N. Toosi University of Technology (2008).

(Manuscript received October 27, 2010,
accepted for publication January 14, 2012.)

https://doi.org/10.1017/jmech.2012.43 Published online by Cambridge University Press